National Water Information System: Web Interface

USGS 15286500 LUCILE C NR WASILLA AK

Available data for this site SUMMARY OF ALL AVAILABLE DATA GO

Stream Site

DESCRIPTION:

Latitude 61°33'40.35", Longitude 149°46'43.53" NAD83
Matanuska-Susitna Borough, Alaska, Hydrologic Unit 19020505
Drainage area: 16.35 square miles
Datum of gage: 190.6 feet above NAVD88.

AVAILABLE DATA:

Data Type	Begin Date	End Date	Count
Field measurements	1981-03-02	2011-08-18	21
Field/Lab water-quality samples	1982-03-10	1983-07-27	3

OPERATION:

Record for this site is maintained by the USGS Alaska Water Science Center
Email questions about this site to Alaska Water Science Center Water-Data Inquiries

U.S. Department of the Interior | U.S. Geological Survey

Title: NWIS Site Information for Alaska: Site Inventory

URL: http://waterdata.usgs.gov/ak/nwis/inventory?

Page Contact Information: Alaska Water Data Maintainer

Page Last Modified: 2012-02-16 12:28:24 EST

0.19 0.17 caww02

SPATIALLY TELESCOPING MEASUREMENTS FOR CHARACTERIZATION OF GROUND WATER – SURFACE WATER INTERACTIONS ALONG LUCILE CREEK, ALASKA

By

Colin P. Kikuchi

A Thesis Submitted to the Faculty of the

DEPARTMENT OF HYDROLOGY AND WATER RESOURCES

In Partial Fulfillment of the Requirements

For the Degree of

MASTER OF SCIENCE

WITH A MAJOR IN HYDROLOGY

In the Graduate College

THE UNIVERSITY OF ARIZONA

2011

STATEMENT BY AUTHOR

This thesis has been submitted in partial fulfillment of requirements for an advance degree at The University of Arizona and is deposited in the University Library to be made available to borrowers under rules of the Library. Brief quotations from this thesis are allowed without special permission, provided the accurate acknowledgement of source is made. Request for permission for extend quotation from or reproduction of this manuscript in whole or in part may be granted by the head of the major department or the Dean of the Graduate College when in his or her judgment the proposed use of the material is in the interest of scholarship. In all other instances, however, permission must be obtained from the author.

SIGNED: __Colin Kikuchi_____

APPROVAL BY THE THESIS DIRECTOR

This thesis has been approved on the date shown below:

_____
Dr. Paul A. Ferré
Professor of Hydrology

_____
November 2nd, 2011

ACKNOWLEDGEMENTS

I gratefully acknowledge the invaluable guidance and support from Steve Frenzel and Dan Long of the USGS Alaska Science Center, and Stan Leake of the USGS Arizona Water Science Center. Colleague reviews by Edward Moran and Donald Rosenberry greatly improved the quality of this manuscript. Ann Marie Larquier, Charles Grammer, and Shamariah Hale provided excellent field assistance. Grey Nearing provided valuable technical support in filtering temperature time series records. Data collection and analysis for this project were generously supported by funding from the Alaska Department of Natural Resources and the U.S. Fish and Wildlife Service. Last but not least, I enthusiastically thank my academic advisor Dr. Ty Ferré for his constant support, encouragement and great ideas.

TABLE OF CONTENTS

TABLE OF CONTENTS - *CONTINUED*

LIST OF FIGURES

LIST OF TABLES

ABSTRACT

The suite of measurement methods available to characterize fluxes between groundwater and surface water is rapidly growing. However, there are few studies that examine approaches to design of field investigations that include multiple methods. We propose that performing field measurements in a spatially telescoping sequence improves measurement flexibility and accounts for hydrologic scale while still allowing for parsimonious experimental design. We applied this spatially telescoping approach in a study of ground water-surface water (GW-SW) interaction during base flow conditions along Lucile Creek, located near Wasilla, Alaska. Catchment-scale data, including channel geomorphic indices and hydrogeologic transects, were used to screen areas of potentially significant GW-SW exchange. Specifically, these data indicated increasing groundwater contribution from a deeper regional aquifer along the middle to lower reaches of the stream. This initial assessment was tested using reach-scale estimates of groundwater contribution during base flow conditions, including differential discharge measurements and the use of chemical tracers analyzed in a three-component mixing model. The reach-scale measurements indicated a large increase in discharge along the middle reaches of the stream accompanied by a shift in chemical composition towards a regional groundwater end member. Finally, point measurements of vertical water fluxes – obtained using seepage meters as well as newer temperature-based methods – were used to evaluate spatial and temporal variability of GW-SW exchange within representative reaches. The spatial variability of upward fluxes, estimated using streambed temperature

mapping at the sub-reach scale, was observed to vary in relation to both streambed composition and the magnitude of groundwater contribution from differential discharge measurements. The spatially telescoping approach improved the efficiency of this field investigation. Beginning the assessment with catchment-scale data allowed us to identify locations of GW-SW exchange, plan measurements at representative field sites and improve interpretation of reach-scale and point-scale measurements.

1. INTRODUCTION

Competing demands for water resources within and between human communities and natural systems necessitates competent, scientifically-based management. Hydrologists have long recognized the interconnection of surface water and ground water (Tóth, 1970; Rushton and Tomlinson, 1979; Meyboom 1967) and the importance of hydrologic processes underpinning the structure and function of aquatic ecosystems (Brunke and Gonser, 1997; Ward *et. al.* 1994). Recent advances in conceptualization of GW-SW interactions are described by Winter *et. al.* (1998) and by Sophocleous (2002) and numerous researchers have developed innovative field methods to quantify interactions between GW-SW; Rosenberry and LaBaugh (2008) provide a review of this body of literature.

Spatial variability of ground water fluxes to surface water is a persistent problem in the characterization of GW-SW interactions at environmentally relevant scales. For example, point measurements of streambed vertical hydraulic conductivity (Genereux *et. al.*, 2008) and seepage (Rosenberry and Pitlick, 2009), may vary by orders of magnitude within a reach resulting in a heterogeneous distribution of vertical fluxes across the streambed. This heterogeneity makes it difficult to determine reach-average fluxes from point measurements, and to predict the magnitude of local vertical streambed fluxes. The location and magnitude of vertical streambed fluxes have important ecological implications; for example, ground water discharge zones provide refugia for salmonids during summer/winter temperature extremes (Hayashi and Rosenberry, 2004).

Hydrologists must strike a reasonable balance between designing field investigations that are robust with respect to multi-scale processes (Dahl *et. al., 2007*), but also practical with respect to the logistical realities of field-based science. Taken together, historically proven techniques and newer measurement approaches provide a wide array of tools to characterize GW-SW interactions. However, the challenge remains in designing field investigations that employ multiple methods to investigate scale dependent hydrologic processes.

This study uses an approach to designing field investigations of GW-SW interaction that considers three elements of field experimental design:

(1) The challenges of matching the inherent scales of processes of interest and the scales of available measurements (***Measurement Scale***);
(2) The restrictions placed on hydrologic measurement and monitoring by time and cost constraints (***Measurement Parsimony***);
(3) The logistical difficulty of adapting field campaigns in the context of recently acquired data (***Measurement Flexibility***).

Using multimodal measurements at nested spatial scales (e.g. Soto-Lopez, 2008) improves the characterization of GW-SW interactions. In this study, a spatially telescoping approach was adopted for planning field investigations. This approach entails beginning the investigation with measurements and analysis at regional spatial scales, and progressively increasing the spatial resolution of field measurements based on both the hydrologic questions of interest and the results of measurements at more coarse spatial

resolution. Such an approach not only improves the accuracy of regional-scale characterization, but also allows for more detailed study of local-scale processes. This approach to field investigation design corresponds quite well to a conceptual framework of GW-SW interactions proposed by Dahl *et. al.* (2007). Specifically, preliminary assessment using both geomorphic features and regional hydrogeology may be used to screen areas of potentially significant GW-SW exchange and to select sites representative of a given "riparian hydrological type" (Dahl *et. al.*, 2007). At those selected sites, reach-integrated hydrometric measurements coupled with chemical tracers may be used to provide quantitative flux estimates and aid in the selection of additional point measurements to characterize the "riparian flow path type" (Dahl *et. al.*, 2007) at the local scale. Designing measurement campaigns to move sequentially from regional to local scales not only allows for flexibility in revising field campaign priorities, but also accounts for nested heterogeneities that are characteristic of the hydrogeologic setting.

In this study, the spatially-telescoping approach was applied to characterize GW-SW interactions for Lucile Creek, situated in hummocky glacial terrain (Winter, 2001) of the Matanuska-Susitna Valley, Alaska. The field campaign described in this report constitutes part of a regional-scale ground water investigation, including hydrogeologic characterization and the development of a groundwater flow model. During the course of this study, it was determined that accurate estimates of water fluxes between ground water and surface water would be valuable both for improving conceptual understanding of hydrogeologic conditions in the study area, and for calibration of the ground water flow model. Lucile Creek was selected for detailed study partly because of its importance

as spawning habitat for salmon in the Big Lake Watershed, and partly for its hydrogeologic setting characteristics, discussed in more detail in the following chapter.

2. STUDY AREA DESCRIPTION

2.1 Location and surface features

The Lucile Creek subwatershed occupies approximately 150 km^2, and is located in the Matanuska-Susitna Valley, near the city of Wasilla in south-central Alaska (figure 1). Lucile Creek originates at the western end of Lucile Lake, flowing approximately 20 km to the confluence with Little Meadow Creek. Lucile Creek receives no known surface water inputs along its course, so any increase in discharge between its upstream and downstream ends is due to ground water discharge into the stream. During summer 2010, the total precipitation was 14.4 cm, and total potential evaporation calculated from measurements at a nearby meteorological station was 39.3 cm. Of the total precipitation, the heaviest rains in the study area typically occur between late July and early September. The ice-free season in the study area typically begins with "break-up" in late April, and ends with "freeze-up" in late October. On the basis of hydrographs from several observation wells, Trainer (1960) proposed that ground water recharge predominantly during and after late summer rains, with some recharge from snowmelt after break-up. The Matanuska-Susitna Valley is the region experiencing the most rapid population growth in the state of Alaska. Current and future residential developments are densely clustered around Wasilla (Gary Prokosh, Alaska Department of Natural Resources, 2009; personal communication) and include rural areas which do not receive city water or sewer service. The potential impact of both distributed ground water pumping and

changing water quality has driven interest in the characteristics of GW-SW interactions along small streams such as Lucile Creek (Curran and Rice, 2009).

2.2 Regional hydrogeology

The Lucile Creek subwatershed occupies glacially dominated terrain deposited in a structural trough located between the Talkeetna Mountains to the north, and the Knik Arm and Chugach Mountains to the south. The Talkeetna Mountains, located approximately 15 km to the north of Lucile Lake, comprise a complex of Mesozoic-age crystalline and metamorphic rocks, overlain by Tertiary-age sedimentary rocks (Wilson *et. al.* 2009). The Chugach Mountains, located approximately 15 km south-southwest of Lucile Lake, include Mesozoic-age metasedimentary and accretionary rocks (Wilson *et. al.*, 2009). Upper Cook Inlet underwent three major glaciations during the Quaternary period (Reger and Updike, 1983), resulting in spatially complex deposition of glacial, fluvial, lacustrine, and estuarine sediments. Wilson *et. al. (*2009) mapped the surficial distribution of unconsolidated sediments deposited during the most recent glaciations. Ground water is present under both confined and unconfined conditions, depending upon local stratigraphy and relations between unconsolidated units. Moran and Solin (2006) compiled and mapped water levels in more than 700 water wells located throughout the Matanuska-Susitna Valley.

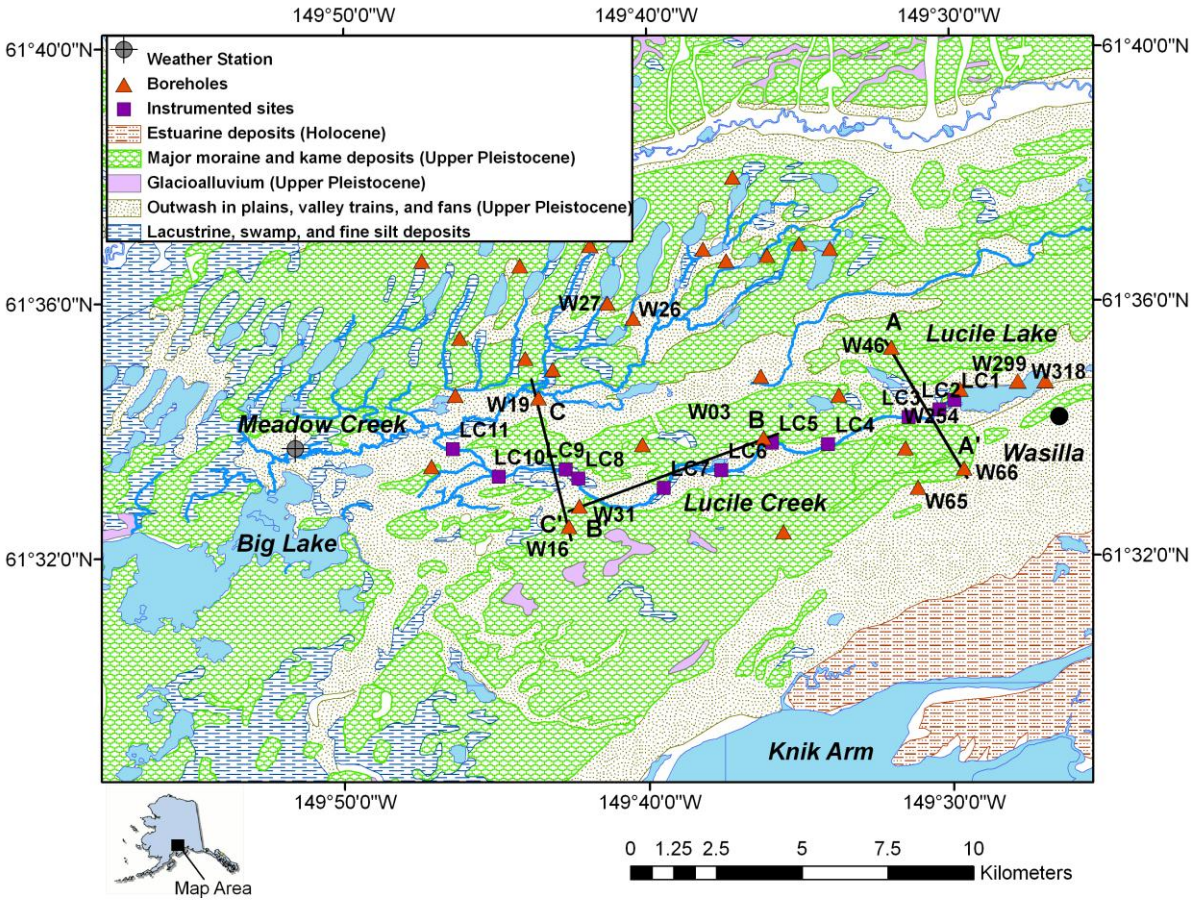

Figure 1. Location of Lucile Creek, Alaska. Figure shows surficial geology (from Wilson *et. al.* 2009) and location of boreholes, transects, and instrumented sites.

The regional-scale water table map shows shallow ground water flowing north-south from the Talkeetna mountains into Knik Arm, with a northeast-southwest component of flow near Big Lake. This water table map agrees well with a similar map produced by Jokela *et. al.* (1991). These authors compiled water levels and geologic information from approximately 3,600 water well logs, and used the results to conceptualize hydrogeology and GW-SW interaction in 11 subwatersheds of the Matanuska-Susitna Valley, including the Lucile Creek subwatershed. From their analysis, they concluded that Lucile Lake

likely receives significant ground water inflows, possibly owing to the seasonal formation of water table mounds on the south shore of the lake. They also noted the presence of multiple closed depressions in the Lucile Creek subwatershed, but found insufficient evidence to characterize the ground water flow system along the course of Lucile Creek.

3. METHODS

3.1 Local hydrogeology

Water fluxes between ground water and surface water are driven, at the broadest spatial scale, by hydrogeology. Dahl *et. al.* (2007) refer to this broader setting as the "landscape type" for GW-SW interactions. For the case of Lucile Creek, geologic transects (figure 2a-c) were used to determine the landscape type. A geologic model of the area near Lucile Creek was constructed using the *RockWorks* ™ software package (Golden, CO) using as input the lithologies reported in 26 shallow (less than 60 m depth) borehole logs adjacent to Lucile Creek; the locations of the boreholes are shown in figure 1. Borehole well casing and selected points along the streambed were measured using Real Time Kinematic (RTK) GPS survey techniques with a Trimble 4700 Receiver (Sunnyvale, CA). Elevations are accurate to 3 cm (Trimble Navigation Limited, 1998). The land surface elevation used in the geologic model was obtained using the National Elevation Dataset for Alaska (U.S. Geological Survey, 2007), which has a 60 m horizontal resolution. Gesch (2007) calculated that NED elevations for the contiguous United States are accurate to 4.84 m; the uncertainty in land surface elevation from the Alaska NED is likely higher, due to the coarse horizontal resolution. Water levels were measured in 26 nearby wells during summer 2009 and summer 2010 for use in local flow direction analysis. The lithologies, land surface elevations, and water levels were linked and defined relative to NAVD88 using the GPS surveyed well head elevations. From this data, selected hydrogeologic transects were constructed, which are shown in figures 2a-c.

3.2 Geomorphology

Geomorphic characteristics have been statistically linked to the regime of GW-SW interactions for alluvial aquifers; in particular, Larkin and Sharp (1992) found that channel sinuosity and channel gradient can be used to infer the relative dominance of underflow (down valley) vs. base flow (riverward) components of the ground water flow direction in alluvial systems. Specifically, alluvial systems with channel sinuosity of less than 1.3 and channel gradient greater than 0.0008 are typically underflow dominated, meaning that ground water does not contribute appreciably to flow in the river. On the basis of these findings, sinuosity and channel gradient were selected for catchment-scale assessment GW-SW interactions along Lucile Creek. The channel thalweg and meander belt axis were obtained by digitizing 2005 NRCS orthophotos (USDA NRCS, 2005) using *ArcGIS* v. 9.0 software package (Redlands, CA). From this dataset, stream sinuosity, *Si*, was then estimated by,

$$Si = l_s / l_b \qquad \textbf{(1)}$$

where l_s is length of the stream along the channel thalweg, and l_b is the length of the meander belt axis (Brice, 1964). The channel gradient, *Sl*, was estimated as,

$$Sl = \Delta z / l_s \qquad \textbf{(2)}$$

where Δz is the difference in elevation between the most upstream and downstream points.

3.3 Physical measurements

During the summer of 2010, stream stages were measured every 15 minutes using KPSI pressure transducers (Pressure Systems Inc., Hampton, VA) at USGS stream gages upstream (USGS Site ID 15286400) and downstream (USGS Site ID 15286500) ends of Lucile Creek. Manual discharge measurements, obtained for different stages with a Pygmy meter and an Aquacalc Pro Computer (JBS Instruments, Sacramento CA), were used to develop rating curves for each gaging station following USGS protocols (Rantz *et. al.* 1982). Streamflow records (figure 3) are available during the summer months (approximately May-October 2010). Synoptic differential discharge measurements (seepage runs) were performed during base flow conditions in October 2009 and May-June, and September 2010 at 8-11 additional locations along the stream. Also during summer 2010, vertical hydraulic gradients were measured at sites selected for this study using a hydraulic potentiomanometer as described by Winter *et. al.* (1988). Seepage meters (0.25 m^2 in area), as described by Rosenberry (2008), were installed in the streambed at instrumented sites to provide direct measurements of vertical water fluxes. The seepage meters were allowed to equilibrate for at least 5 days before the first measurements were taken. Each seepage meter was equipped with a 2 m hose leading to a 4 liter freezer storage bag, housed in a bag shelter to minimize the effects of stream velocity and bag removal on seepage measurements. Change in seepage bag mass was measured from June to October 2010 using an Ohaus Model CT6000 Portable Balance (Parsippany, NJ). A bag correction factor of 0.95 was applied to each calculated flux as suggested by Rosenberry and Menheer (2006). Meteorological data – including

measurements of rainfall, temperature, wind speed and direction, relative humidity, barometric pressure, and incoming/outgoing short wave radiation – available from a nearby weather station were used to estimate potential evaporation using methods described by Shuttleworth (1993) (figure 4).

3.4 Environmental tracers

Specific conductance was measured periodically from June-October 2010 using a Hach Sension5 meter (Loveland, CO) at each of the eight seepage meter locations. At each measurement time, the meter was allowed to stabilize for 5 min before recording the measured value. Stream water samples were collected synoptically at each of the eight seepage meter locations in June 2010, and ground water samples were collected from domestic wells (W26, W27, W31, and W65) during summer 2010. Prior to sampling, the wells were purged by evacuating water until at least three casing volumes had been removed, and temperature and specific conductance stabilized. Surface water and ground water samples were stored in sealed polyethylene bottles and analyzed for $\delta^{18}O$ and δD at the ENRI Stable Isotope Laboratory at the University of Alaska, Anchorage using a Picarro L2120 Isotopic Water Analyzer (Sunnyvale, CA).

Two sites – in reaches identified as losing by the October 2009 seepage run – were chosen for the installation of thermistor arrays; these data were used to obtain point estimates of water fluxes. At each site, Onset Computer Co. Tidbit thermistors (Bourne, MA) were deployed at 0, 10, and 20 cm depth in the streambed. A hollow steel tube was driven into streambed sediments to the desired depth, and a thermistor inserted through

the tube. The tube was removed while holding the thermistor in place with a wooden rod, allowing the streambed sediments to collapse around the thermistor. The thermistor arrays were deployed for 34 days in June-August 2010. Additional thermistors were deployed at the streambed surface for all sites at which streambed temperature mapping was conducted. All thermistors used during this study were calibrated against a reference National Institute of Standards and Technology calibrated mercury thermometer.

Time-series temperature records obtained from the thermistor arrays were processed using a cosine taper band-pass filter as described by Hatch *et. al.* (2006), with water flux computed as a function of either amplitude ratio, A_r, or phase shift, $\Delta\phi$ between pairs of streambed thermistors,

$$v_{Ar} = \gamma\left[\frac{2\kappa_e}{\Delta z}\ln A_r + \sqrt{\frac{\alpha - v^2}{2}}\right] \quad \textbf{(3a)}$$

$$v_{\Delta\phi} = \gamma\left[\sqrt{\alpha - 2\left(\frac{\Delta\phi 4\pi\kappa_e}{P\Delta z}\right)^2}\right] \quad \textbf{(3b)}$$

Where γ is the ratio of streambed and fluid volumetric heat capacities, Δz is the spacing between the thermistors, κ_e is the effective thermal diffusivity, v is the thermal front velocity, and $\alpha = \sqrt{v^4 + \left(8\pi \cdot \frac{\kappa_e}{P}\right)^2}$, where P is the period of temperature fluctuation. Values for streambed thermal parameters were taken from Hatch (2006) and are displayed in table 1. Both (3a) and (3b) were programmed in the MATLAB environment to be solved recursively with a convergence criterion of 10^{-4} m s^{-1}. Hatch *et. al.* (2006) suggest that the detectable limits and sensitivities be estimated when calibrating water

fluxes; specifically, that only seepage velocities resulting in $\frac{dAr}{dvf} \geq 10^{-3}$, be considered valid with equation (3a). The calculated fluxes over the 34 day measurement period were above the detectable limits for each pair of streambed thermistors.

To examine spatial variability of ground water discharge through the streambed within gaining reaches, streambed temperature mapping campaigns were performed over a three-day period in June according to the method described by Schmidt *et. al.* (2007). Assuming a quasi-steady-state temperature boundary condition in the stream water, mapped streambed temperatures were used to calculate the upward water flux q_z with an analytical solution to the heat flow equation:

$$q_z = -\frac{K_{fs}}{\rho_f c_f z} ln \frac{T(z)-T_L}{T_0-T_L} \quad \textbf{(4)}$$

where K_{fs} is the thermal conductivity of the solid-fluid system, $\rho_f c_f$ is the volumetric heat capacity of the solid-fluid system, *z* is the depth of the temperature measurement, *T(z)* is the temperature at depth *z*, T_L is the ground water temperature, and T_0 is the mean surface water temperature at the streambed (*z*=0). The parameter values used for this case are shown in table 1. To estimate the mean surface water temperature T_0 and test the quasi-steady-state assumption, Onset Comp. Co. Tidbit thermistors were deployed near the locations of streambed temperature mapping for approximately 20 days. During the three-day measurement campaign, streambed temperatures were measured at 20 cm depth at 98 points in the stream (approximately 10-20 per site) using either an Oakton (Vernon Hills, IL) or a Cole Parmer Digisense ThermologR thermometer (Vernon Hills, IL) with

the probe housed in a thin (<2 cm) perforated metal tube. One to three streambed temperature measurements were taken at transects across the stream channel, with those transects located at approximately 5 m intervals.

Hydraulic Properties	**Value**	**Thermal Properties**	**Value**
Porosity[a], n [-]	0.45	Volumetric heat capacity of fluid[b], $\rho_f c_f$, [J m^3 K^{-1}]	4.19×10^6
		Volumetric heat capacity of the streambed[c], ρc [J m^3 K^{-1}]	2.99×10^6
		Ratio of streambed to fluid heat capacity, γ [-]	0.71
		Thermal conductivity of saturated sediments[b], K_{fs} [J s^{-1} m^{-1} K^{-1}]	2.0
		Thermal dispersivity[d], β [m]	1.0×10^{-3}

[a]Estimated from qualitative observation of the sediments and literature values.
[b]From Stonestrom and Blasch (2003)
[c]Computed using $\rho c = n(\rho_f c_f + (n-1)(\rho_s c_s)$, with $\rho_s c_s$=2.0 J m^3 K^{-1}
[d]From Hatch *et. al.* (2006)

Table 1. Parameters used for flux calculations from streambed temperature mapping and time-series temperature records.

4. RESULTS

The measurements described above were performed in a spatially telescoping sequence, beginning with catchment-scale measurements and ending with the point-scale measurements at instrumented field sites. The results obtained during each phase of the investigation were used to guide selection of measurement locations in subsequent phases. The results are described within the spatially telescoping framework to better illustrate the way in which measurements performed at increasingly fine spatial scales were guided by the results of previous, coarser-scale measurements.

4.1 Local hydrogeology

Lucille Creek flows through a low-relief topographical depression filled by Quaternary-age glacial outwash deposits, interbedded with some lacustrine and swamp deposits in isolated areas. On either side of this local depression are moraine, kame, and esker deposits. Qualitatively, transect A-A' replicates this spatial pattern; for example, transect A-A' shows that the topographic depression cuts through an unconfined (water-table), sandy gravel (interpreted here as outwash) aquifer, and is bounded from above by dry, mounded diamict (interpreted here as glacial till deposits). Transect A-A' shows that the till layer overlies a deeper confined, water-bearing gravel formation. On the basis of the water level in borehole W46, which rises above the top of the deeper gravel/sandy gravel formation, the till is interpreted as a confining layer. Transect B-B' is approximately parallel to Lucile Creek, crossing the stream channel near site LC8. Similar to transect A-A', this transect indicates a confined aquifer beneath and surrounding Lucile Creek;

however, the sandy clay confining layer is spatially discontinuous. Near piezometer W03, the regional aquifer appears to be directly in contact with the riparian aquifer. It is therefore likely that regional ground water, flowing through the regional gravel/sandy gravel aquifer at 50-80 m elevation, exchanges with water in the shallower riparian aquifer at and around this location. Transect C-C' crosses Lucile Creek approximately 2 km downstream from field site LC8. Piezometer W19 penetrates a shallow unconfined (water-table) aquifer comprising sandy gravel, with the water table gradually sloping south to north in this area. Similar to transect A-A', transect C-C' shows outwash deposits associated with Lucile Creek and Little Meadow Creek separated by glacial till. However, in this case, the glacial till is less hummocky than in transect A-A'.

The geomorphic indices and hydrogeologic conceptualization based upon existing catchment-scale data provide a starting point for characterizing the landscape type and riparian hydrogeologic type. From the longitudinal evolution of channel sinuosity, it was hypothesized that ground water contribution would likely be focused between sites LC6-LC11 (8.8-20.7 km downstream of Lucile Lake). From hydrogeologic transects, a likely zone of contact between regional/riparian aquifer systems was identified between sites LC6-LC7 (8.8-11.43 km downstream of Lucile Lake). These catchment scale data indicate an area of potentially significant GW-SW interaction between sites LC6-LC7. Reach-scale measurements were then used to test these hypotheses based upon catchment-scale measurements. Specifically, the relative contribution of water from the riparian and regional aquifer system was investigated using environmental tracers

(section 4.3), and the expected transition from underflow to mixed-flow conditions was investigated with differential discharge measurements (section 4.4)

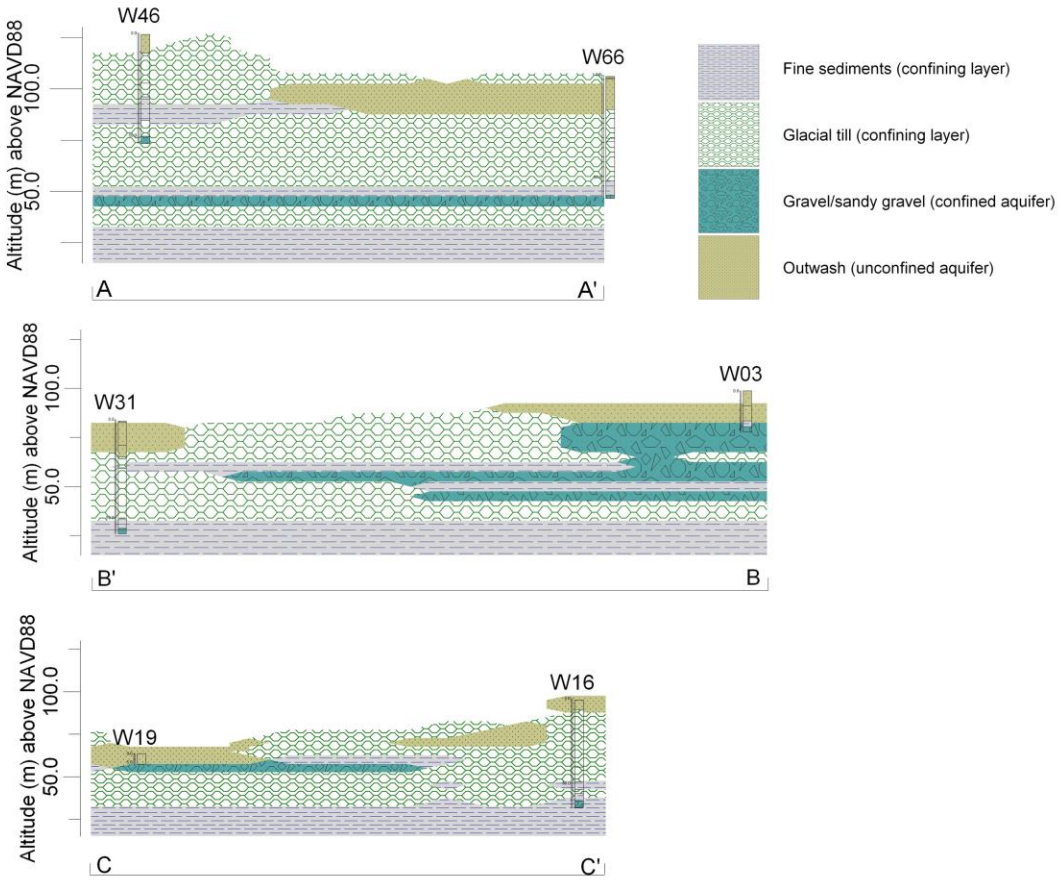

Figure 2. Geologic cross sections (a) A-A', (b) B-B', and (c) C-C'. The bottom of the regional, confined aquifer is arbitrarily set to the bottom of boreholes used in the model construction; however, this zone may in fact extend much deeper.

4.2 Geomorphology

The streambed elevation of Lucile Creek drops 40.5 m over approximately 20.7 km, resulting in a channel gradient of 0.002. Streambed elevation was measured with high

vertical accuracy only at the upstream and downstream ends of the stream, and therefore reach-specific channel gradient values are not available. The distances measured along the channel thalweg, l_s, and the meander belt axis, l_b, are 20.7 km and 17.8 km respectively, resulting in a sinuosity of 1.16 for the entire stream. Calculated sinuosities for distinct reaches are displayed in table 2, and show sinuosity to increase from 1.1 to 1.26 between sites LC6 and LC8. In the framework of Larkin and Sharp (1992), these results indicate negligible ground water contribution to Lucile Creek. However, the depositional environment for Lucile Creek is very different from those environments considered by Larkin and Sharp (1992); for example, Curran and Rice (2009) observed that channel attributes for streams occupying similar topographic and geomorphic terrain to Lucile Creek are influenced primarily by glacial landforms.

Reach number	Starting point	End point	l_s [km]	l_b [km]	Sinuosity [-]
1	LC1	LC3	1.74	1.66	1.05
2	LC3	LC4	2.82	2.63	1.07
3	LC4	LC5	2.1	1.82	1.15
4	LC5	LC6	2.12	1.93	1.1
5	LC6	LC7	2.65	2.11	1.26
6	LC7	LC8	3.79	3.16	1.2
7	LC8	LC11	5.5	4.43	1.24

Table 2. Stream sinuosity, computed for reaches of Lucile Creek.

To contrast, the alluvial systems studied by Larkin and Sharp (1992) were more influenced by regional topography, following a predictable transition in sediment load from bedload to suspended load moving from upstream to downstream reaches. It is therefore conceivable that the sinuosity values determined by Larkin and Sharp (1992) as indicators of ground water flow direction might be different in value for the case of a

small, uniformly low-velocity (current less than 0.4 m s^{-1}) stream such as Lucile Creek. If indeed ground water flow direction is correlated with sinuosity for this system, ground water contribution would likely be focused between sites LC6-LC11. This assessment was tested using reach-scale measurements of ground water-surface water interaction (sections 4.3-4.4).

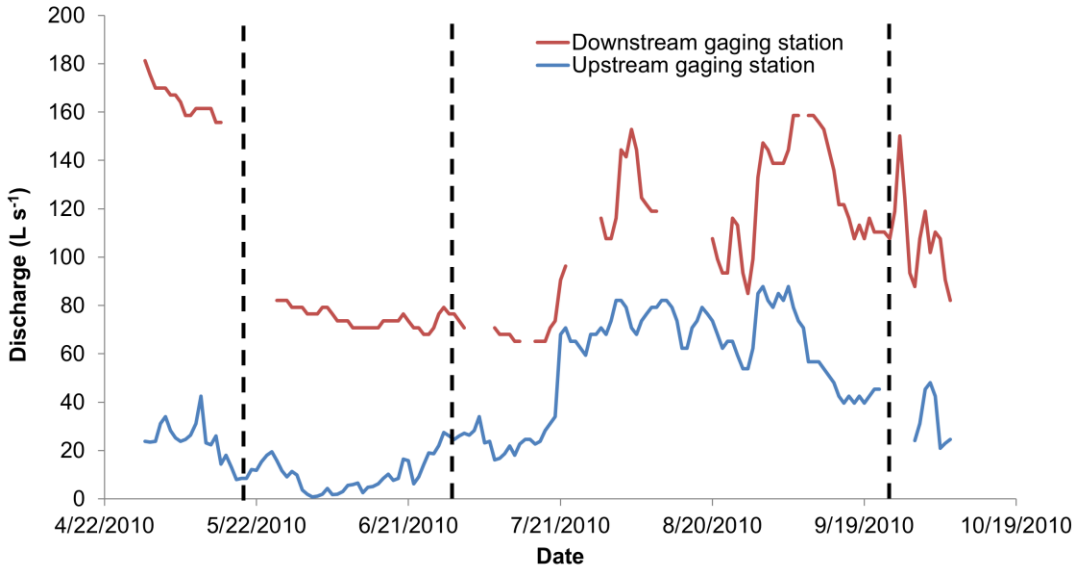

Figure 3. Hydrographs from upstream (below Lucile Lake, USGS Site ID 15286400) and downstream (near confluence with Little Meadow Creek, USGS Site ID 15286500) gaging stations. Black dotted lines indicate timing of differential discharge measurements.

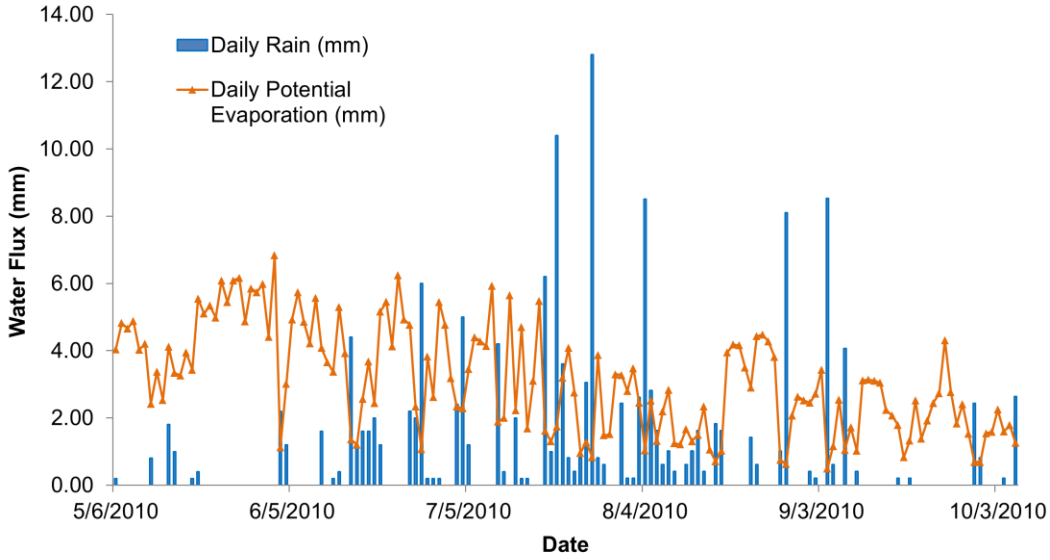

Figure 4. Daily rain and potential evaporation during measurement campaign, based on measurements from nearby weather station.

4.3 Tracer-based measurements

Catchment-scale data suggested three likely sources of water to Lucile Creek: Lake Lucile, the riparian aquifer, and the regional aquifer. Water at the upstream end of Lucile Creek (site LC1) originates from Lucile Lake, with $\delta^{18}O$ and δD values of -11.89 and -108.97‰ respectively. The isotopic composition of stream waters from Lucile Creek changes progressively moving downstream, with $\delta^{18}O$ and δD values of -14.80 and -121.91‰ measured in water samples from site LC8, 15.2 km downstream of Lucile Lake. The isotopic composition of ground water sampled from the riparian and regional aquifers is not different at the 5% significance level, and cannot be used to statistically discern which aquifer contributes water to the stream. Nonetheless, ground water samples obtained from riparian and regional aquifers have mean $\delta^{18}O$ values of -16.16

and -15.57‰ respectively, so ground water input from one of these aquifers may explain the longitudinal change in isotopic composition of stream water.

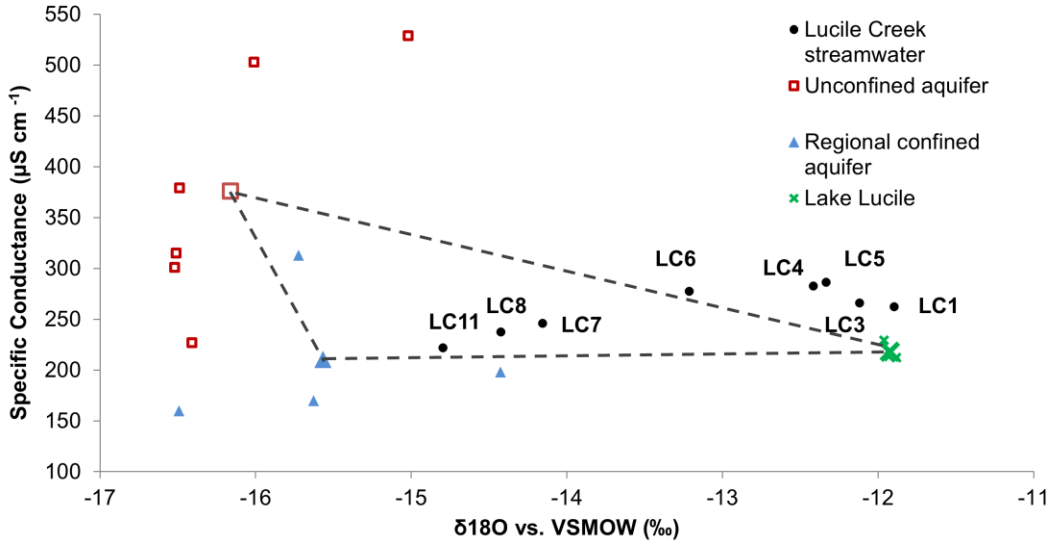

Figure 5. Specific conductance vs. $\delta^{18}O$ of surface and ground water sampled during summer 2005 and summer 2010. Small symbols represent individual water samples; large symbols represent mean values for each end member group. Dashed lines represent the envelope of mixing trend. Ground water samples from the confined aquifer were obtained at wells W26, W27, W31, and W65 during summer 2010. Ground water samples from the unconfined aquifer were obtained from wells W254, W318, and W299 during summer 2005 (Moran and Solin, 2006).

Specific conductance of surface water and ground water was used to aid the determination of water sources in Lucille Creek under the assumption of distinct chemical composition for each end member in the system. The mean specific conductance of stream water in Lucile Creek, measured during base flow conditions in June-July 2010, increased from 262 to 283 µS/cm along the upstream reach (0-6 km), and decreased from 283 to 222 µS/cm along the downstream reach (6-21 km). The specific conductance of ground water from the regional aquifer (mean = 210 µS/cm) and

riparian aquifer (mean = 376 µS/cm) differs at the 5% significance level. Specific conductance is not a conservative tracer and it is possible that in-stream or sub-surface processes may be responsible for changes in specific conductance along Lucile Creek. Under the assumption of sufficiently conservative chemical behavior in this system, specific conductance may be used as a second tracer to distinguish between water originating from regional and riparian aquifers. The distinct end member values, combined with the observed gradual increase in specific conductance from 0-6 km, indicate that riparian aquifer is likely the source of ground water input to Lucile Creek along the upstream reaches. Decreasing specific conductance along the mid-stream and downstream reaches (6-21 km) indicates that the regional aquifer is likely the source of ground water input along these reaches. Using $\delta^{18}O$ and specific conductance as chemical tracers in a three-component mixing model (figure 5), it was estimated that at the confluence with Little Meadow Creek the relative contribution of water from Lucile Lake, the riparian aquifer, and the regional aquifer are approximately 22%, 6%, and 72%, respectively. Error in estimated ground water contribution by this method would be dominated primarily by uncertainty in the specific conductance of the groundwater end members, which exhibit some variation about the mean value.

4.4 Differential Discharge Measurements

During summer 2010, a net gain in discharge ranging from 23.0 to 157.0 L s^{-1} was observed over the entire length of Lucile Creek. Despite distinct discharge values at the farthest upstream measurements, the discharge measured at the downstream location (20

km) clusters around the same value of 100 L s^{-1} for each of the three seepage runs. These results suggest that downstream discharge is largely independent of the inflow to the stream from Lucile Lake. Synoptic differential discharge measurements show the longitudinal variability in reach-scale base flow gain in discharge (figure 6).The largest increase in discharge occurs from 10-15 km downstream of Lucile Lake. It was therefore estimated that that on a broad spatial scale, Lucile Creek gains between 45-75% of its discharge from ground water. A three-component mixing model using $\delta^{18}O$ and specific conductance suggests that at the downstream end, the majority of this upwelling ground water is from the regional aquifer.

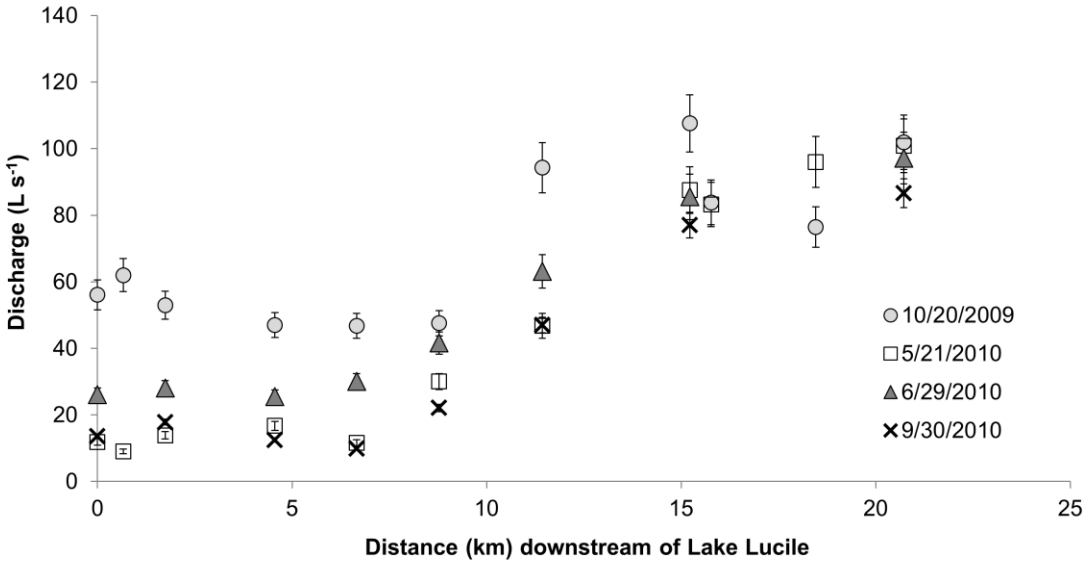

Figure 6. Measured discharge along the length of Lucile Creek; with the exception of those from 9/30/2010, all measurements were performed during baseflow conditions. Error bars depict 8% error.

Coupling hydrometric and tracer-based, reach-scale measurements allowed us to identify sections of Lucile Creek that receive significant ground water input. These results supported the initial characterization based on catchment-scale measurements. The reach-scale measurements do not provide information about hydrologic processes at the sub-reach scale, such as the riparian flow path type; however, reach-scale measurements were used to guide selection of point-scale measurements. Specifically, point-scale measurements of fluxes and gradients were compared to reach-scale measurements of normalized fluxes (section 4.5). Next, streambed temperature mapping (section 4.6) was used to investigate spatial variability of upward fluxes in gaining reaches, and streambed temperature time series methods (section 4.7) were used to further investigate suspected losing reaches.

4.5 Point-scale physical measurements

Seepage meters at eight sites along Lucile Creek were used to directly measure water fluxes from June-October 2010 and compute mean water fluxes during base flow conditions. For reaches identified as strongly gaining, point measurements using seepage meters were used to infer whether ground water discharge is diffuse and uniform or focused at buried springs (e.g. Becker *et. al.*, 2004). For sites LC1, LC4, and LC8, mean water fluxes detected using seepage meters were inconsistent with one or more

	Mean flux [L m^{-2} d^{-1}]				
Site	**Seepage Meter**	**Thermistor array**	**Streambed temperature mapping**	**Measured hydraulic gradients [-]**	**Hydraulic conductivity [cm/s]**
LC1	-1.70E-02	--	--	-8.97E-02 1.71E-02	-- --
LC3	1.53E-01	--	1.51E+02	8.00E-03	2.22E-05
LC4	1.00E-01	-4.39E+04	--	-7.16E-02 -3.19E-01	-- --
LC5	2.84E-01	--	6.32E+01	--	--
LC6	7.78E+01	--	1.88E+02	2.83E-02 9.43E-02	3.18E-03 --
LC7	-1.73E-01	--	2.01E+02	6.14E-02 1.10E-01 1.63E-01	-- -- --
LC8	1.79E-02	-5.435E+04	--	6.45E-04 -4.10E-02	-- --
LC11	2.69E-01	--	1.23E+01	0.00E+00 4.76E-03	-- 6.55E-05

Table 3. Summary of point measurements from instrumented sites along Lucile Creek. Reported mean fluxes from seepage meter measurements are representative of a three-week measurement period (6/22/2010-7/12/2010) at fixed points, and mean fluxes from streambed temperature mapping are representative of a three-day measurement period (6/22/2010-6/24/2010) along multiple transects upstream and downstream of seepage meters.

measurements of hydraulic gradient (table 3). One explanation for the observed inconsistencies is temporal variability in vertical fluxes. Water flux measurements with seepage meters integrate vertical fluxes over time, since the time elapsed between consecutive measurements of bag mass can be on the order of hours, days, or even weeks.

On the other hand, measurements of hydraulic gradient are representative of a five minute measurement period and are practically point measurements in time. It is conceivable that the fluxes at sites LC4 and LC8 are highly variable in time; such temporal variability was observed by Rosenberry and Pitlick (2009). It is also possible that hydraulic gradient and seepage measurements at this site correspond to different flow patterns in the streambed.

Rosenberry and Pitlick (2009) observed similar inconsistency between the direction of hydraulic gradient and seepage, which they attribute to local-scale effects associated with hyporheic exchange near the sediment-water interface. In either case, the observed inconsistencies between measurement types at introduce uncertainty into our assessment of the riparian flow path type at sites LC1, LC4, and LC8. Therefore, we do not include gradient/seepage measurements at these sites in our analysis. For the remaining seepage measurements, the streambed vertical hydraulic conductivity may be estimated using measured baseflow flux and hydraulic gradients. These calculated values (table 3) range from 10^{-5} to 10^{-3} cm s^{-1}, and are consistent with qualitative field observations of streambed texture.

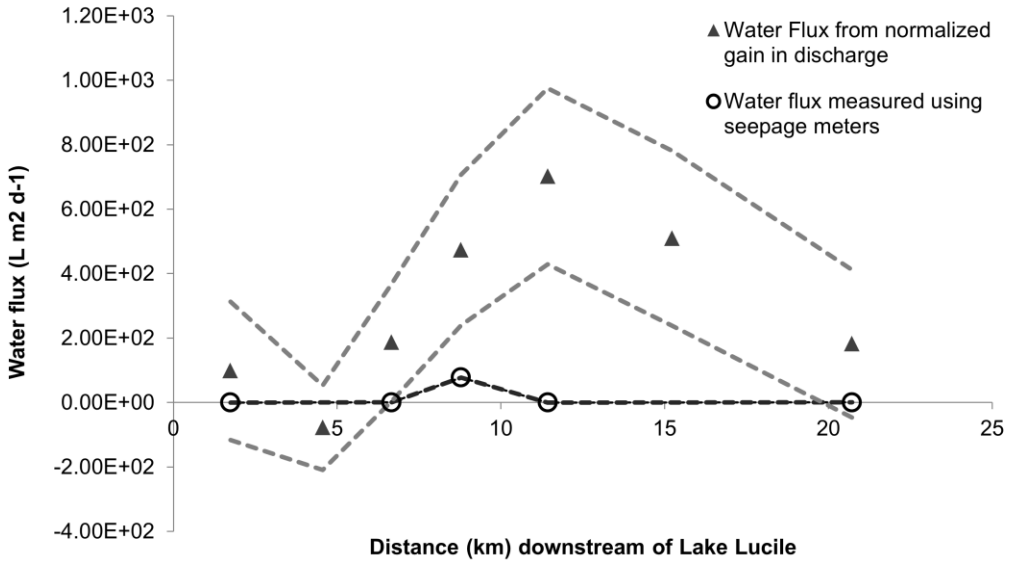

Figure 7. Areally-normalized stream-aquifer water fluxes, as measured by seepage meters (circles) and differential discharge measurements (triangles). Dashed lines represent upper and lower error bounds for both measurement types.

The mean water fluxes from seepage meters and the normalized apparent baseflow gain are displayed in figure 7. The error bounds for the mean fluxes were established by computing the upper and lower boundaries of each individual seepage measurement associated with bag mass measurement error, and calculating the mean of both upper and lower values over the baseflow period. When upper and lower bounds for the normalized fluxes are calculated using the measurement error for each method, it becomes apparent that in reaches approximately 7-15 km below Lucille Lake, estimated fluxes from the seepage meters deviate significantly from those estimated by differential discharge. This is also the section where most of the gains in discharge occur. The inability of measured fluxes in seepage meters to match these observed gains suggests that ground water discharge along this section of the stream is focused at buried springs or through the stream banks. Streambed temperature mapping (Schmidt *et. al*, 2007) was used to test this explanation; the results are presented below (section 4.6). If, in fact, ground water discharge is direct (localized in the streambed) rather than diffuse, then point-scale vertical flux measurements should be spatially variable.

4.6 Point measurements – Streambed temperature mapping

The temperature of shallow ground water measured upgradient of Lucile Creek was 3.9°C over the three-day temperature mapping campaign. Ground water temperatures from the regional confined aquifer as measured in nearby piezometers varied by less than 0.6°C from this value. Measured stream water temperatures during this period ranged from 7.4 to 21.3°C, with a large drop in mean water temperature between sites 4-5 (table

4). Based on the results of the reach-scale measurements, it was hypothesized that the drop in temperature corresponds with the increasing dominance of the ground water component in discharge as suggested from the reach-integrated measurements. To better resolve the spatial variability of upwelling water fluxes between sites, both mean stream temperature and descriptive statistics for streambed temperatures at each site are presented in table 4. The mean stream temperature over the 3-day mapping period drops sharply between LC5 and LC6; the mean upward water flux computed using equation (3) and the coefficient of variation (CV) for those values are largest at sites LC6 and LC7.

				Computed upward water fluxes ($L\ m^{-2}\ d^{-1}$)		
Site	**Distance (km) downstream**	**Mean water temperature T_0, (°C)**	**Number of measurements**	**Range**	**Mean**	**Coefficient of Variation**
LC3	1.74	16.3	12	38.5-368.8	151.12	0.76
LC5	6.66	16.2	8	36.7-94.0	63.22	0.30
LC6	8.78	10.3	15	44.3-748.4	188.12	1.06
LC7	11.43	10.8	19	57.1-761.2	200.89	0.99
LC11	20.72	10.6	12	0.3-19.8	12.35	0.57

Table 4. Site-by-site descriptive statistics for upward water fluxes, computed using streambed temperature measurements.

The locations of mapped streambed temperatures at sites LC6 and LC7 are shown in figures 8a-b. These sites show the largest spatially integrated water fluxes over the entire stream; that is, they encompass the majority of the ground water discharge. Observations of spatial variability in water fluxes through the streambed are therefore particularly important at these sites. Examining the mapped streambed temperatures in plan view,

some clear spatial patterns are apparent. At site LC6, the largest water fluxes occur on the north side of the stream; in particular, the computed fluxes for points on the easternmost meander were of 548 and 749 L m^{-2} d^{-1}. At site LC7, the spatial pattern of fluxes appears less clear. Fluxes of roughly similar magnitude were computed along the same transect for most of the points, suggesting less variation across the channel. The two largest computed fluxes (561 and 761 L m^{-2} d^{-1}) are observed in the channel thalweg near the center of site LC7; however, there are smaller fluxes of 62 and 186 L m^{-2} d^{-1} located at the upstream end of the site. Coupling the differential reach-scale measurements with mapped streambed temperatures, it was observed that the spatial variability of ground water discharge is highest in reaches where the reach-scale ground water discharge is highest.

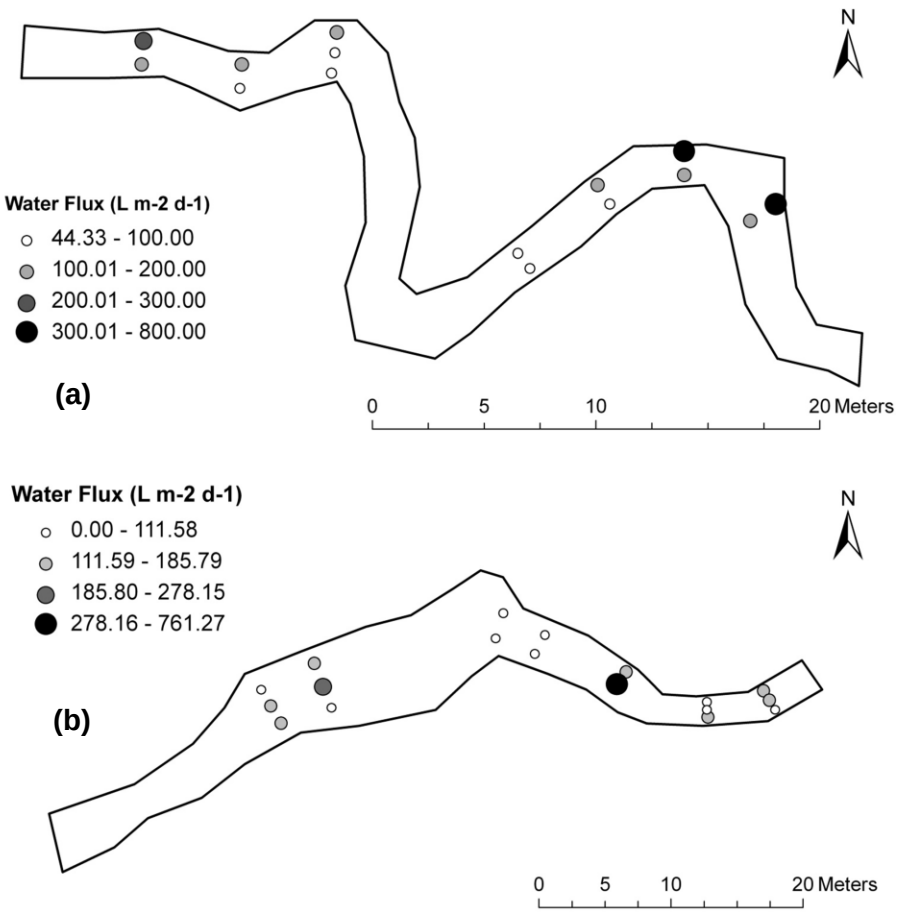

Figure 8. GW-SW fluxes at sites (a) LC6 and (b) LC7, computed from streambed temperatures at 20 cm. Locations are approximate.

Sites LC6 and LC7 demonstrate the largest reach-scale ground water discharge in the stream. These sites exhibit distinct spatial distributions of water fluxes as obtained from streambed temperature mapping; at site LC6 (CV=1.06), higher fluxes were observed on the north side of the channel, and no clear pattern was observed for site LC7 (CV=0.99). Finally, the mean fluxes estimated from streambed temperature mapping are consistently several orders of magnitude higher than those from seepage meters (table 4). These differences are attributed to the greater spatial coverage of streambed temperature

measurements, which increased the likelihood of measuring vertical flux over a preferential flow path.

4.7 Point measurements – Time-series streambed temperatures

Differential discharge measurements indicated discharge losses in excess of the measurement error from 4-7 km (sites LC1-LC4) and 15-18 km (sites LC8-LC10) during October 2009, but not during June 2010. Downward hydraulic gradients also were observed at these sites. These results suggest that the stream may be losing water to the riparian aquifer along these two sections. To test this interpretation of the seepage run data, the method of Hatch *et. al.* (2006) was applied to time-series streambed temperature data from sites 4 and 8. Due to sensor loss, time-series temperature data only were available at 0 cm and 10 cm depth at each site. Nevertheless, this sensor spacing is sufficient to detect water fluxes within a given range, depending on streambed thermal and hydraulic properties (Hatch *et. al.*, 2006). The resulting values for water fluxes at sites LC4 and LC8, over the 34-day thermistor deployment, are displayed in figure 9. These fluxes fall within the detectable limits described in section 3.4, and therefore are considered reliable observations.

The local flux measurements are comparable to the apparent discharge losses observed between sites LC1-LC4. The areally normalized downward water flux, calculated from October 2009 discharge measurements, was 170.21 L m^2 d^{-1} between sites 1-4. The computed water flux from the thermistor array at site LC4 ranged from -149.47 to -

730.08 L m^2 d^{-1} over the June-July 2010 measurement period, bracketing the spatially integrated water flux from October 2009 discharge losses.

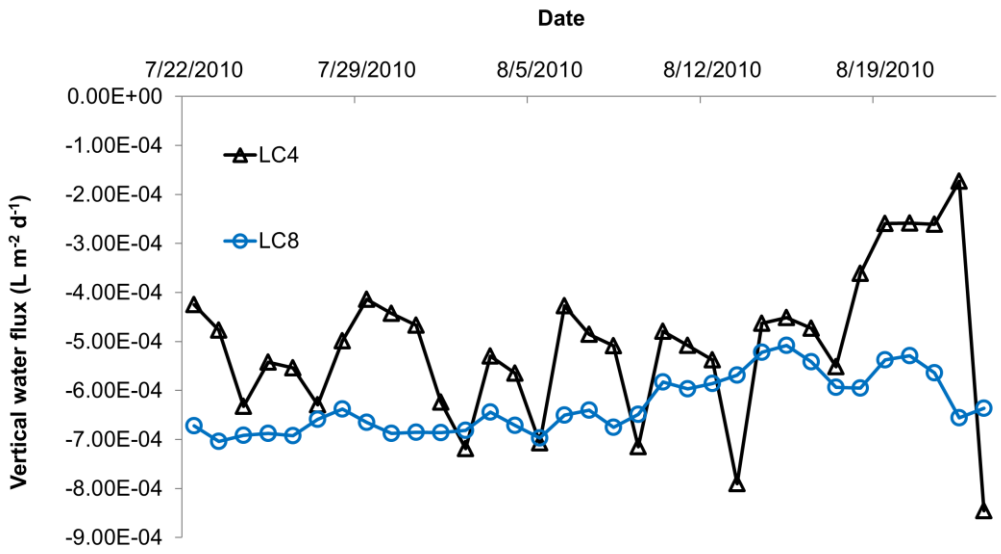

Figure 9. Water fluxes at sites LC4 and LC8, computed using amplitude ratios of filtered temperatures at 0-10 cm depth in the streambed.

The application of the temperature time-series method in this case therefore provides an additional line of evidence for the initial characterization of discharge losses between sites LC1-LC4. However, these results contradict the fluxes measured using seepage meters near (within 50 m) of where the thermistor arrays were deployed; mean fluxes using seepage meters at these points were both upward. The seepage meters at these sites were deployed slightly deeper (20-40 cm) than the streambed temperature sensors; therefore, it is conceivable that the inconsistency between measured flux direction may again be attributed to contrasting flow patterns associated with different depths in the streambed.

5. DISCUSSION

5.1 The spatially telescoping approach

The experimental design described here includes multiple measurements performed in a spatially telescoping sequence, designed to improve the information provided by each subsequent, smaller-scale measurement by selecting those measurements on the basis of results from previous, larger scale measurements. This approach to characterizing GW-SW interactions allows for consideration of spatially-variable processes while reducing costs from instrumentation and labor. Along these lines, this approach is evaluated by its ability to achieve **(1) *measurement parsimony***, **(2) *measurement flexibility***, and address **(3) *measurement scale***. Finally, results from this investigation are synthesized to classify GW-SW interactions along Lucile Creek according to the typology of Dahl *et. al.* (2007).

5.2 Catchment-scale to reach-scale measurements

Sinuosity values close to 1.3 were observed along the downstream reaches of Lucile Creek (table 2), suggesting that ground water contributes to the stream along these reaches. Local hydrogeology indicates the presence of a riparian aquifer in direct contact with the stream, and a deeper regional aquifer, confined in places by a layer of glacial till and lenses of silty clay. The two aquifers are likely hydraulically connected between sites LC6-LC7, where these confining layers are spatially discontinuous. The catchment-scale data indicate that ground water may contribute significantly to the stream between sites LC6-LC8; however, these data do not indicate whether water from the regional aquifer is in fact entering the riparian aquifer, and furthermore cannot be used to screen areas of

potential stream loss to ground water. Both of these issues were resolved through the use of reach-scale measurements– differential discharge and sampling of stream water and ground water– to test the initial catchment-scale characterization of GW-SW interactions. This series of telescoping measurements exemplifies **measurement parsimony**: selecting measurements at the next level of spatial resolution based on their ability to test prior conceptualization of the system and provide new information. Longitudinal increases in discharge and evolving chemical composition of stream water – consistent with three-component mixing – indicate that ground water inputs to the stream beginning at approximately 15 km downstream of Lucile Lake are supplied by the regional aquifer, supporting the initial conceptualization based on hydrogeologic transect B-B'. Reach-scale measurements also provided new information by identifying losing reaches of the stream.

5.3 Reach-scale to point-scale measurements

The improved spatial resolution provided by reach-scale measurements aids in selecting point measurement methods to be applied at individual field sites. For example, fluxes obtained from streambed time-series data are least sensitive to measurement error in losing reaches (Shanafield *et. al.*, unpublished results), and streambed temperature mapping may only be used to compute vertical water fluxes in gaining conditions. Therefore, accurate reach-scale characterization of GW-SW interactions allows for **measurement flexibility** in selecting point scale measurements.

Streambed temperature mapping was performed at five sites for which differential discharge and hydraulic gradient measurements indicated gaining conditions. The streambed temperature mapping method assumes that all water fluxes are upward; observed upward hydraulic gradients and water fluxes – measured using seepage meters – at those five sites lends credence to that assumption. For all sites, the coefficient of variation (CV) of upward vertical fluxes increased proportional to the normalized spatially-integrated water flux obtained from differential discharge measurements (table 2). In this analysis, sites LC3, LC6 and LC11 were selected to represent the riparian flow path type for upstream, mid-stream, and downstream sites. Between sites LC3 and LC6, a 383% increase in the normalized flux, $\bar{q}$, is accompanied by a 40% increase in the CV. To contrast, a 61% reduction in normalized flux between sites LC6 and LC11 is accompanied by a 46% decrease in the CV.

These results may be explained by considering the factors that contribute to the spatial variability of water fluxes. Kalbus *et. al.* (2009) showed that the homogeneous streambeds have the effect of reducing the CV of upward vertical water fluxes by up to 137% in comparison to heterogeneous streambeds, even when the mean hydraulic conductivity and mean flux are held constant. For the case of Lucile Creek, the observed spatial variability of upward vertical fluxes may be attributed to hydraulic properties of the streambed. Hydrogeologic transects B-B' and C-C', corresponding approximately with sites LC6 and LC11, show that the riparian aquifer comprises similar geologic material at both sites. However, qualitative observations of streambed sediments at the two sites differ tremendously. A wide range of materials from gravel and rocks to sand,

silty/clayey sand, and organics were observed in the streambed at site LC6; to contrast, the streambed at site LC11 comprises gravel, cobbles, and pebbles, with few, if any, fine sediments observed.

The observed changes in the CV of upward vertical fluxes between sites may be explained by variability in streambed composition and structure. At upstream and mid-stream reaches (0-15 km), spatial variability in vertical water fluxes is likely controlled by independent heterogeneity between the streambed and the riparian aquifer. At the farthest downstream reach (15-22 km), the controlling influence of aquifer heterogeneity upon vertical fluxes is moderated by a relatively homogeneous streambed. This moderating influence may be complemented by hyporheic flow induced from larger bedform amplitude (e.g. Tonina and Buffington, 2007) and streambed hydraulic conductivity, diminishing the signal of the apparent vertical flux from streambed temperature measurements. This interpretation can be used to distinguish between apparent *direct* and *diffuse paths* for sites LC6 and LC11 respectively. Using point-scale measurements to characterize the riparian flow path type addressed **measurement scale,** as these measurements were performed at spatial scales that are comparable to the hydrologic process of interest.

5.4 Hypothesized Typology of GW-SW Interaction

Investigation of the local hydrogeology surrounding Lucille Creek indicates the presence of two aquifers. Valley train outwash deposits constitute local, unconfined aquifers. At greater depth, permeable sand and gravel deposits overlain by glacial till and form

regional confined aquifers. The *regional hydrogeological setting* is therefore described as "a three-unit system consisting of an unconfined aquifer, a confining layer, and a confined aquifer (Dahl *et. al.*, 2007)." Geologic transects constructed from local borehole lithologies indicate three contact types between the regional and local aquifers. The two aquifers are disconnected at reaches 0-6 km downstream, and 15-22 km downstream of Lucile Lake. In the mid-stream reaches at 6-15 km, confined contact transitions into bottom regional contact. With respect to riparian hydrogeological type, the upper reach of Lucile Creek is classified as confined (type 2) and the middle/lower reaches as unconfined regional (type 8)/unconfined local (type 7), according to the typology of Dahl *et. al.* (2007). On the basis of hydrogeologic evidence and the longitudinal evolution of stream water composition, outflow from Lucile Lake in the headwaters of Lucile Creek is supplemented by upwelling ground water from the regional ground water body along the middle reaches. The riparian flow path type describes water fluxes from the local riparian aquifer to the stream, and therefore classifies GW-SW interactions at the finest spatial scale. The Lucile Creek sub-catchment is relatively pristine, with no drains (i.e. flow path Q_4) present to bypass the local aquifer. Furthermore, no tributaries were observed to contribute water to the stream by overland flow (i.e. flow path Q_2). The riparian flow path type is therefore some combination of diffuse (Q_1) and direct flowpaths (Q_3). During the 3-day streambed temperature mapping campaign, high spatial variability in vertical water fluxes was observed at sites LC3 and LC6, suggesting direct flowpaths from the riparian aquifer into the stream. It should be noted that the composition of stream water differs between these two sites, with the former dominated more by water from the local

unconfined aquifer, and the latter by water from the regional confined aquifer. In comparison, very low variability was observed at site LC11, indicating diffuse riparian flowpaths. Streambed composition was qualitatively observed to differ between sites LC3/LC6 and LC11, with the latter characterized as relatively homogeneous with no observed deposits of organics or fine sediments. It is therefore hypothesized that streambed composition, coupled with the disconnection of regional and local aquifers, might explain the apparent diffuse flowpaths for site LC11.

6. CONCLUSION

A variety of measurement techniques are available to estimate water fluxes between ground water and surface water at distinct spatial scales. Previous studies (e.g. Cey *et. al.*, 1998) have found that point measurements are typically less reliable than reach-integrated measurements in estimating ground water discharge due to geologic heterogeneity. However, point-scale measurements are valuable for investigating hydrologic processes occurring at sub-reach scales, such as distinct riparian flow-path types. Field measurements were performed along Lucile Creek in a spatially telescoping sequence to guide efficient selection of field sites for reach-scale and point-scale measurements. Catchment-scale characterization of geomorphology and hydrogeology suggests increasing mixed-flow to base flow dominance beginning about 6-km downstream of Lucile Lake, and approximates the location of contact zones between regional and local aquifers.

The initial assessment of GW-SW interaction along Lucile Creek was tested using two types of reach-integrated field measurements. Differential discharge measurements taken during base flow episodes suggest ground water flux to the stream from 6-15 km downstream of Lucile Lake, a reach of the stream with no tributary inputs. Stream water samples, analyzed for specific conductance and stable isotopes of water, indicate that stream water at reaches 0-6 km below Lucille Lake moves initially toward a local, unconfined end member and at reaches 6-15 km moves toward a regional, confined end member. This result is subject to uncertainty in the specific conductance of ground water

from regional and local aquifers, exhibited by the spread in ground water specific conductance values in figure 5. The differential discharge measurements support the interpretation that longitudinally increasing stream sinuosity corresponds with increased ground water exchange with the stream. At the same time, the hydrogeologic conceptualization is supported by longitudinal evolution of stream chemistry observed during base flow conditions. Integrating catchment and reach-scale measurements allows for classification of regional hydrogeologic setting and contact type between regional and local aquifers. Finally, these results were used to select sites for point measurements of vertical water fluxes across the streambed. Quantitative measurements of flux, however, are subject to errors owing to violation of underlying assumptions (e.g. vertical upward water flux for streambed temperature mapping), and errors related to the measurement technique (e.g. sediment compaction near seepage meters). Including multiple types of measurements at a given spatial scale provides a means for assessing the relative error in each measurement type. For example, measurements of hydraulic gradients were used to identify sites where streambed temperature mapping data could not be used to compute water fluxes, due to the violation of the upward flow assumption required for the analytical solution.

Spatial heterogeneity in the subsurface complicates the characterization of GW-SW interactions; this often has the effect of limiting the available level of detail that may be accurately considered. However, conducting multimodal field measurements in a spatially-telescoping sequence allows for the consideration of multi-scale processes, from water exchange between distinct hydrologic units to flow paths within a relatively small

segment of a riparian system. Therefore, this approach is useful in multi-scale classification of GW-SW interactions (e.g. Dahl *et. al.* 2007). Furthermore, this approach constrains the number of measurements that are necessary to accurately characterize such multi-scale processes, reducing the costs of labor and equipment during field measurement campaigns.

APPENDIX A: MATLAB CODE USING HATCH'S SOLUTION TO COMPUTE VERTICAL WATER FLUX

```
%% Colin Kikuchi, October 2010
%% University of Arizona, Department of Hydrology and Water Resources
%% A script to compute water fluxes from streambed temperature data, using the
solution
%% of Hatch et. al. 2006 with amplitude ratio and phase shift as inputs

% First, the peaks of each time series are identified
%%********BEGIN
PROGRAM**********************************************************
clear all
close all
clc
%%********USER
CONTROL**********************************************************
load johnsonrd_filtered
int1=15;                  %Sampling interval (min), top sensor
int2=2;                   %Sampling interval (min, bottom sensor
%z1_raw=z0_recon_filt;         %Raw temperature time series, top sensor
%z2_raw=z10_recon_filt;        %Raw temperature time series, bottom sensor
z1=z_0_filtered;             %Filtered temperature time series, top sensor
z2=z_10_filtered;             %Filtered temperature time series, bottom sensor
t1=water_day;              %Time vector, top sensor
t2=water_day_10;              %Time vector, bottom sensor
%%********TASKS/COMPUTATIONS*************************************
**********
pd1=1440/int1;
pd2=1440/int2;
ndays1=length(z1)/pd1;
ndays2=length(z2)/pd2;
days=min(ndays1,ndays2);
%
%Peak picking for each day and each temperature time series. For the
%following, column 2 is the daily temperature peak, and column 1 is the
%corresponding time (in water day).
peaks_z1(1,2)=max(z1(1:pd1,1));
peaks_z1(1,1)=t1(find(z1(1:pd1,1)==max(z1(1:pd1,1))));
peaks_z2(1,2)=max(z2(1:pd2,1));
peaks_z2(1,1)=t2(find(z2(1:pd2,1)==max(z2(1:pd2,1))));
%

for aa=1:floor(days)-1
```

```
    start1=pd1+1+((aa-1)*pd1);
    stop1=start1+pd1-1;
    peaks_z1(aa+1,2)=max(z1(start1:stop1));
    peaks_z1(aa+1,1)=t1(find(z1==max(z1(start1:stop1))),1);
    %
    start2=pd2+1+((aa-1)*pd2);
    stop2=start2+pd2-1;
    peaks_z2(aa+1,2)=max(z2(start2:stop2));
    peaks_z2(aa+1,1)=t2(find(z2==max(z2(start2:stop2))),1);
    %

end
% Next, the amplitude ratio and phase shift (in days) are computed
for cc=1:floor(days)-1
    Ar(cc)=peaks_z2(cc,2)/peaks_z1(cc,2);
    delta_phi(cc)=peaks_z2(cc,1)-peaks_z1(cc,1);
end
%
% Finally, the Hatch solution is solved iteratively, using both inputs of
% amplitude ratio and phase shift.
% --------------------User-defined inputs---------------------------------
delta_z=0.1;                %Distance between sensors (m)
n=0.45;                     %Porosity of streambed sediments
P=86400;                    %Period of fluctuation (seconds)
ndays=floor(days)-1;        %Number of days considered in calculation
v(1:ndays,1)=-1e-5;         %Thermal front velocity (m/s), this is the starting value
nn_Ar=1;                    %Counter used to track recursive solution (Ar)
nn_dp=1;                    %Counter used to track recursive solution (delta-phi)
rho_c=(n*4.19e6+(n-1)*2.0e6);   %Volumetric heat capacity of the streambed
gamma=rho_c/4.19e6;         %Ratio of streambed to fluid volumetric heat capacity
lambda_0=2.0;               %Thermal conductivity of streambed (J/(smK))
beta=0.001;                 %Thermal dispersivity of streambed (m)
conv_crit=5e-4;             %Convergence criterion (m/s)
                            %K_e is effective thermal diffusivity,
                            %(m2/s)
inst_res=0.02;              %Sensor resolution, degrees C
% ------------------------------------------------------------------------
[v_Ar,v_dp,K_e,alpha,dAr_dvf,vAr_type]=hatch_recursive(ndays,v,Ar,delta_phi,P,lamb
da_0,rho_c,beta,delta_z,conv_crit,gamma);
%
%Lower flux envelope
n=0.25;
rho_c=(n*4.19e6+(n-1)*2.0e6);
gamma=rho_c/4.19e6;
```

```
[v_Ar_lower,v_dp_lower,K_e,alpha,dAr_dvf_l,vAr_type_l]=hatch_recursive(ndays,v,Ar,
delta_phi,P,lambda_0,rho_c,beta,delta_z,conv_crit,gamma);
%
%Upper flux envelope
n=0.7;
rho_c=(n*4.19e6+(n-1)*2.0e6);
gamma=rho_c/4.19e6;
[v_Ar_upper,v_dp_upper,K_e,alpha,dAr_dvf_u,vAr_type_u]=hatch_recursive(ndays,v,A
r,delta_phi,P,lambda_0,rho_c,beta,delta_z,conv_crit,gamma);

%
figure
line(t1,z1,'color','b')
hold on
line(t2,z2,'color','g')
plot(peaks_z1(:,1),peaks_z1(:,2),'ok')
plot(peaks_z2(:,1),peaks_z2(:,2),'ok')
xlabel('Water Day')
ylabel('Filtered temperature, degrees C')
legend('z=0 cm','z=10 cm')

figure
plot(1:ndays,Ar,'ob')
%
figure
plot(1:ndays,delta_phi,'xk')
%
figure
plot(1:ndays,v_Ar(:,3),'--b');
hold on
xlabel('Day')
ylabel('Fluid velocity (cm/s)')
%
figure
plot(vAr_type(:,1),vAr_type(:,3),'-.b');
axis([-3e-5 2e-5 0 1])
xlabel('Seepage Velocity (m/s)')
ylabel('Amplitude ratio')
figure
semilogy(vAr_type(:,1),dAr_dvf(:,1),'-k');
line([-5e-4 5e-4],[1e-3 1e-3]);
axis([-5e-4 5e-4 1e-10 1e6])
xlabel('Seepage velocity (m/s)')
ylabel('Derivative, dAr/dvf')
```

Subroutine “hatch_recursive.m”

```
function
[v_Ar,v_dp,K_e,alpha,dAr_dvf,vAr_type]=hatch_recursive(ndays,v,Ar,delta_phi,P,lamb
da_0,rho_c,beta,delta_z,conv_crit,gamma,inst_res);
%% keywords: water flux, temperature time series, streambed temperature
%% [v_Ar,v_dp,K_e,alpha,dAr_dvf,vAr-type]=hatch_recursive(ndays,v,Ar,delta_phi,P
%% ,lambda_0,rho_c,beta,delta_z);
%% This function estimates stream-aquifer water flux for a thermistor array
%% with instrument and streambed thermal/hydraulic properties specified in
%% the master script, recursively calculating thermal front velocity for
%% inputs of amplitude ratio and phase shift.
%% Colin Kikuchi, Mat-Su GW Study
%% MATLAB 7.8.0(R2009a)
%%------------------------------------------------------------------------
%The thermal front velocity as a function of amplitude ratio, v_Ar
nn_Ar=1;
for dd=1:ndays
   vf=v*gamma;
   K_e=lambda_0/rho_c+beta*abs(vf(dd,1));
   alpha(dd,1)=sqrt((v(dd,1)^4)+(8*pi*(K_e/P))^2);
   v_Ar(dd,1)=(2*K_e/delta_z)*log(Ar(dd))+sqrt((alpha(dd,1)+v(dd,1)^2)/2);
   while abs(v_Ar(dd)-v(dd))>conv_crit
      Ar_iter_record(nn_Ar,dd)=v_Ar(dd,1);
      v(dd,1)=v_Ar(dd,1);
      K_e=lambda_0/rho_c+beta*abs(vf(dd,1));
      alpha(dd,1)=sqrt((v(dd,1)^4)+(8*pi*(K_e/P))^2);
      v_Ar(dd,1)=(2*K_e/delta_z)*log(Ar(dd))+sqrt((alpha(dd,1)+v(dd,1)^2)/2);
      fprintf(strcat('Amplitude ratio iteration number ',num2str(nn_Ar),'\n'));
      nn_Ar=nn_Ar+1;
   end
end
%
%----------Screening for detectable velocities----------------------
%The type curve for amplitude ratio is generated using eqn (4b) from Hatch
%et. al. 2006, to screen the estimated fluid velocities and "peg" them at
%the appropriate value.
vAr_type(:,1)=[-5e-4:10e-7:5e-4];
vAr_type(:,2)=vAr_type(:,1)/gamma;
for ff=1:length(vAr_type)
   Ke_type=lambda_0/rho_c+beta*abs(vAr_type(ff,1));
   alpha_type=sqrt((vAr_type(ff,2)^4)+(8*pi*(Ke_type/P))^2);
```

```
    vAr_type(ff,3)=exp((delta_z/(2*Ke_type))*(vAr_type(ff,2)-
sqrt((alpha_type+(vAr_type(ff,2))^2)/2)));
end
%
for gg=2:length(vAr_type)
    dAr_dvf(gg,1)=(vAr_type(gg,3)-vAr_type(gg-1,3))/(vAr_type(gg,1)-vAr_type(gg-
1,1));
end

%The type curve is used to estimate the lower and upper vf limits that are
%detectable over the Ar range defined by instrument resolution.

v_Ar(:,2)=v_Ar(:,1)*gamma;          %Converting from thermal front velocity to fluid
velocity
v_Ar(:,3)=v_Ar(:,2)*100;            %m/s to cm/s

%
% Reset intial value for thermal front velocity
clc
v(1:ndays,1)=-1e-5;
nn_dp=1;
%The thermal front velocity as a function of phase shift, delta_phi
for ee=1:ndays
    K_e=lambda_0/rho_c+beta*abs(vf(dd,1));
    alpha(ee,1)=sqrt((v(ee,1)^4)+(8*pi*(K_e/P))^2);
    v_dp(ee,1)=sqrt(alpha(ee,1)-2*((delta_phi(ee)*4*pi*K_e)/(P*delta_z))^2);
    while abs(v_dp(ee,1)-v(ee,1))>conv_crit
        v(ee,1)=v_dp(ee,1);
        K_e=lambda_0/rho_c+beta*abs(vf(dd,1));
        alpha(ee,1)=sqrt((v(ee,1)^4)+(8*pi*(K_e/P))^2);
        v_dp(ee,1)=sqrt(alpha(ee,1)-2*((delta_phi(ee)*4*pi*K_e)/(P*delta_z))^2);
        dp_iter_record(nn_dp,ee)=v_dp(ee,1);
        fprintf(strcat('Delta_phi iteration number ',num2str(nn_dp),'\n'));
        nn_dp=nn_dp+1;
    end
end

% The computed thermal front velocities are adjusted by gamma
v_dp(:,2)=v_dp(:,1)*gamma;          %Thermal front velocity to fluid velocity
v_dp(:,3)=v_dp(:,2)*10;             %m/s to cm/s
```

REFERENCES

Becker, M.W., Georgian, T., Ambrose, H., Siniscalchi, J., Fredrick, K., 2004, Estimating flow and flux of ground water discharge using water temperature and velocity, 296, p. 221-233.

Brice, J.C., 1964, Channel patterns and terraces of the Loup rivers in Nebraska. U.S. Geological Survey, Professional Paper 422-D.

Brunke, M. and Gonser, T., 1997, The ecological significance of exchange processes between rivers and ground-water, *Freshwater Biol, 37*, 1-33,.

Cey, E.E., Rudolph, D.L., Parkin, G.W., Aravena, R., 1998, Quantifying ground water discharge to a small perennial stream in southern Ontario, Canada, *J. Hydrol., v. 210*, p. 21-37.

Curran, J.H., and Rice, W.J., 2009, Baseline channel geometry and aquatic habitat data for selected streams in the Matanuska-Susitna Valley, Alaska: U.S. Geological Survey Scientific Investigations Report 2009-5084, 24 p.

Dahl, M., Nilsson, B., Langhoff, J.H., Refsgaard, J.C., 2007, Review of classification systems and new multi-scale typology of ground water-surface water interaction, *J. Hydrol. 344*, 1-16.

Dahm, C.N., Grimm, N.B., Marmonier, P., Valett, M.H., Vervier, P., 1998, Nutrient dynamics at the interface between surface waters and ground waters, *Freshwater Biol, 40*, 427-451,.

Genereux, D.P., Leahy, S., Mitasova, H., Kennedy, C.D., Corbett, D.R., 2008, Spatial and temporal variability of streambed hydraulic conductivity in West Bear Creek, North Carolina, USA, *J. Hydrol. 358*, 332-358,.

Gesch, D.B., 2007, Chapter 4 – The National Elevation Dataset, in Maune, D., ed., Digital Elevation Model Technologies and Applications: The DEM Users Manual, 2nd edition: Bethesda, Maryland, American Society for Photogrammetry and Remote Sensing, p. 99-118.

Hatch, C.E., Fisher, A.T., Revenaugh, J.S., Constantz, J., Ruehl, C., 2006, Quantifying surface water-ground water interactions using time series analysis of streambed thermal records: Method development, *Water Resour. Res.,42,* W10410, doi:10.1029/2005WR004787.

Hayashi, M., and Rosenberry, D.O., 2002, Effects of ground water exchange on the hydrology and ecology of surface water: Ground Water, v. 40, no. 3, p. 309-316.

Jokela, J.B., Munter, J.A., and Evans, J.G., 1991, Ground-water resources of the Palmer-Big Lake area, Alaska: A conceptual model: Alaska Department of Natural Resources Division of Geological and Geophysical Surveys Report of Investigations 90-4, 38 p., 3 sheets, scale 1:25,000.

Kalbus, E., Schmidt, C., Molson, J.W., Reinstorf, F., and Schirmer, M., 2009, Influence of aquifer and streambed heterogeneity on the distribution of ground water discharge: Hydrology and Earth System Sciences, v. 13, p. 69-77.

Larkin, R.G., and Sharp, J.M., 1992, On the relationship between river-basin geomorphology, aquifer hydraulics, and ground-water flow direction in alluvial aquifers, *GSA Bulletin, 104,* p. 1608-1620.

Langhoff, J.H., Rasmussen, K.R., Christensen, S., 2006, Quantification and regionalization of ground water-surface water interaction along an alluvial stream, *J. Hydrol, 320,* p. 342-358.

Malcolm, I.A., Soulsby, C., Youngson, A.F., Petry, J., 2003, Heterogeneity in ground water-surface water interactions in the hyporheic zone of a salmonid spawning stream, *Hydrol. Process., 17,* 3, 601-617.

Meyboom, P., 1967, Mass transfer studies to determine the ground water regime of permanent lakes in hummocky moraine of western Canada, *J. Hydrol., 5*, 2, 117-142,.

Moran, E.H., and Solin, G.L., 2006, Preliminary water-table map and water-quality data for part of the Matanuska-Susitna Valley, Alaska, 2005; U.S. Geological Survey Open-File Report 2006-1209, 43 p.

Poole, G.C., Stanford, J.A., Running, S.W., Frisell, C.A., 2006, Multiscale geomorphic drivers of ground water flow paths: subsurface hydrologic dynamics and hyporheic habitat diversity, *J. N. Am. Benth. Soc., 25*, 2 288-303.

Rantz, S.E., and others, 1982, Measurement and computation of streamflow: Volume 1. Measurement of Stage and Discharge. U.S. Geological Survey Water-Supply Paper 2175, 313 p.

Reger, R.D., and Updike, R.G., 1983, Physiographic map and index to field localities of the Upper Cook Inlet area, Alaska: *in* Pewe, T.L. and Reger, R.D., editors, Guidebook to permafrost and Quaternary geology along the Richardson and Glenn Highways between Fairbanks and Anchorage, Alaska, Fourth International Conference on Permafrost: Alaska Division of Geological and Geophysical Surveys Guidebook 1.

RockWorks 15(Revision 2011.3.30)[Software], 2011, Golden Co USA: RockWare, Inc. Available from http://www.rockware.com/

Rosenberry, D.O., 2008, A seepage meter designed for use in flowing water: Journal of Hydrology, v. 359, p. 118-130.

Rosenberry D.O., and LaBaugh, J.W., 2008, Field techniques for estimating water fluxes between surface water and ground water, U.S. Geological Survey Techniques and Methods Report 4-D2.

Rosenberry, D.O., and Menheer, M.A., 2006, A system for calibrating seepage meters used to measure flow between ground water and surface water: U.S. Geological Survey Scientific Investigations Report 2005-5053, 21 p.

Rosenberry, D.O., and Pitlick, J., 2009, Local-scale variability of seepage and hydraulic conductivity in a shallow gravel-bed river, *Hydrol. Process.*, 23, 2206-3318.

Rushton KR, Tomlinson LM, 1979, Possible mechanisms for leakage between aquifers and rivers, *J Hydrol., 40*, 49-65.

Schmidt, C., Conanat, B., Bayer-Raich, M., 2007, Evaluation and field-scale application of an analytical method to quantify ground water discharge using mapped streambed temperatures. *J. Hydrol., 347*, 292-307.

Shuttleworth, W.J., In: Maidment, D.R. (ed.), 1993, Handbook of Hydrology, McGraw-Hill, New York

Sophocleous, M., 2002, Interactions between ground water and surface water: the state of the science, *Hydrogeol. J.*, 10, 52-67.

Soto-López, C.D., 2008, Spatial and temporal variability of vertical hydrologic fluxes at the San Pedro River, AZ. M. Sc. Thesis. University of Arizona, USA.

Stonestrom, D.A., Blasch, K., 2003, Determining temperature and thermal properties for heat-based studies of surface-water ground-water interaction, *U.S. Geol. Surv. Circ., 1260,* 73-80.

Tóth, J., 1970, A conceptual model of the ground water regime and the hydrogeologic environment, *J. Hydrol., 10*, 2, 164-176.

Tonina, D., Buffington, J.M., 2007, Hyporheic exchange in gravel bed rivers with pool-riffle morphology: Laboratory experiments and three-dimensional modeling. *Water Resourc. Res. v. 43*, W01421.

Trainer, F.W., 1960, Geology and ground-water resources of the Matanuska Valley Agricultural Area: U.S. Geological Survey Water-Supply Paper 1494, 116 p.

Trimble Navigation Limited, 1998, 4700 Receiver Operation Manual. Version 1.0, Part Number 36238-00, Revision B.

U.S. Department of Agriculture Natural Resources Conservation Service, 2005, Matanuska-Susitna Borough: U.S. Department of Agriculture Natural Resources Conservation Service, 1-meter orthoimagery.

U.S. Geological Survey, 2007, National Elevation Dataset (NED) – Shaded Relief – Direct Download. Available at URL: http://ned.usgs.gov/

Ward, J.V., Stanford, J.A., Voelz, N.J., 1994, Spatial distribution patterns of Crustacea in the flood plain aquifer of an alluvial river, *Hydrobiologia, 287,* 11-17.

Wilson, F.H., Hults, C.P., Schmoll, H.R., Haeussler, P.J., Schmidt, J.M., Yehle, L.A., Labay, K.A., 2009, Preliminary geologic map of the Cook Inlet Region, Alaska: U.S. Geological Survey Open-File Report 2009-1108.

Winter, T.C., LaBaugh, J.W., Rosenberry, D.O., 1988, Design and use of a hydraulic potentiomanometer for direct measurements of differences in hydraulic head between ground water and surface water, *Limnology and Oceanography*, 33, 5, 1209-1214.

Winter, T.C., Harvey, J.W., Franke, O.L., Alley, W.M., 1998, Ground water and surface water – a single resource. U.S. Geological Survey Circular 1139.

Winter, T.C., 2001, The Concept of Hydrologic Landscapes, *J. Am. Water Res. Assoc., 37*, 2, 335-349.

Lucile Creek Investigation Plan

Title: Lucile Creek groundwater-surface water interaction.

Principal Investigator(s): Steven A. Frenzel, USGS Alaska Science Center.

Objectives: The objective of this study is to determine the spatial and temporal extent of exchange between local groundwater and surface water in Lucile Creek between Lake Lucile and Big Lake Road. The degree to which water is exchanged between groundwater and surface water has a bearing on how water may be adjudicated for instream flow reservations.

Justification: Streamflow in most natural systems is a combination of surface runoff and subsurface, or groundwater discharge to the stream channel. Therefore, management of water resources must consider sources and uses of both groundwater and surface water. In Lucile Creek, the relative contribution of groundwater is believed to be large, but has not been documented. By comparing streamflow on a continuous basis at two locations with no known tributaries between them, the magnitude and seasonal distribution of groundwater contributions can be evaluated. More detailed information about specific areas of groundwater exchange may be gained by using heat as an indicator of groundwater flux. Typically, groundwater will be cooler than surface water during the summer and warmer during other seasons.

Background: The Matanuska-Susitna Valley is the fastest growing area in Alaska. Nearly all new homes or communities in the area rely on groundwater for their domestic water supply. The Alaska Department of Natural Resources has funded the USGS to conduct a study of the groundwater resources in the Matanuska-Susitna Valley to help them better manage the water resources. The major product to be delivered from that project will be a groundwater flow model. Information gained from a more focused effort on groundwater-surface water exchange in Lucile Creek will be used in the model development.

The USGS has extensive experience in monitoring streamflow. Standard procedures are used in establishing monitoring sites and in field techniques and are well documented by the USGS. Currently, the USGS operates more than 120 such sites in Alaska. One site on Lucile Creek, near the outlet of Lake Lucile is being operated as part of the larger study of groundwater in the Matanuska-Susitna Valley, which will continue through 2011.

Procedures: A new streamgage will be established on Lucile Creek where it is crossed by Big Lake Road (see map below). The gage will be instrumented to record stream stage every 15 minutes and will transmit that data to http://nwis.waterdata.usgs.gov/ak/nwis/current/?type=flow. A stage-discharge relation will be developed through routine site visits and once a sufficient relation is developed, discharge, as well as stage, will be reported in real time. In water year 2010, 4-5 discharge measurements will be made at the new streamgage and in water year 2011 6-8 discharge measurements will be made. Because Lucile Creek is relatively small, discharge will be measured with mechanical current meters mounted on a wading rod. Water temperature also will be monitored at 15-minute intervals and reported to the same web site as stage and discharge data.

Groundwater flux in Lucile Creek will be determined through seepage runs and through the use of thermisters placed at multiple depths and distributed longitudinally between the two streamgages. Seepage runs are accomplished by hydrographers measuring stream discharge at numerous locations between the two streamgages in as short a time frame as possible. All visible inflows and outflows from the main stream channel are measured as well. Identical techniques and equipment will be used when measuring discharge during seepage runs as when measuring discharge at the streamgages. Seepage runs

will be made at a minimum following spring snowmelt and in the fall before freeze-up.
The thermisters or temperature loggers that will be used have an accuracy of 0.2 ^{o}C and 1 minute per week. The techniques for use of thermisters or temperature loggers as a means of documenting groundwater flux in streams are described in Rosenberry and LaBaugh (2008). We will follow these techniques and place thermisters at approximately 10 and 20 centimeter depths vertically beneath the streambed at three locations along Lucile Creek during July 2010. Data will be retrieved from the loggers in September 2010 and June 2011.

Products: Streamflow and water temperature data from the streamgage on Lucile Creek at Big Lake Road will be published and archived in the National Water Information System data base, which is publicly accessible through the USGS web site. The seepage run measurements also will be archived there as miscellaneous measurements. Groundwater flux data will be incorporated in the report describing results of the larger groundwater study funded by the Alaska Department of Natural Resources, which will be published in 2012.

Schedule:

June 2010	Install streamgage on Lucile Creek at Big Lake Road
June 2010-Sept 2011	Operate streamgage
July 2010	Conduct seepage run and install thermisters in Lucile Creek
Sept 2010	Conduct seepage run and download data loggers
June 2011	Download data loggers

References:

Rosenberry, D.O., and LaBaugh, J.W., 2008, Field techniques for estimating water fluxes between surface water and ground water: U.S. Geological Survey Techniques and Methods 4-D2, 128 p.

Google maps Address **Wasilla, AK**